HHS Public Access

Author manuscript

J Bone Miner Res. Author manuscript; available in PMC 2015 April 25.

Published in final edited form as:

J Bone Miner Res. 2011 August ; 26(8): 1883–1890. doi:10.1002/jbmr.401.

Fibroblast Growth Factor 23 Regulates Renal 1,25-Dihydroxyvitamin D and Phosphate Metabolism via the MAP Kinase Signaling Pathway in *Hyp* Mice

Daniel Ranch, **Martin YH Zhang**, **Anthony A Portale**, and **Farzana Perwad**

Department of Pediatrics, University of California San Francisco, San Francisco, CA, USA

Abstract

In X-linked hypophosphatemia (XLH) and in its murine homologue, the *Hyp* mouse, increased circulating concentrations of fibroblast growth factor 23 (FGF-23) are critical to the pathogenesis of disordered metabolism of phosphate (P_i) and 1,25-dihydroxyvitamin D [$1,25(OH)_2D$]. In this study, we hypothesized that in *Hyp* mice, FGF-23-mediated suppression of renal $1,25(OH)_2D$ production and P_i reabsorption depends on activation of mitogen-activated protein kinase (MAPK) signaling. Wild-type and *Hyp* mice were administered either vehicle or the MEK inhibitor PD0325901 (12.5 mg/kg) orally daily for 4 days. At baseline, the renal abundance of *early growth response 1* (*egr1*) mRNA was approximately 2-fold greater in *Hyp* mice than in wild-type mice. Treatment with PD0325901 greatly suppressed *egr1* mRNA abundance in both wild-type and *Hyp* mice. In *Hyp* mice, PD0325901 induced an 8-fold increase in renal *1α-hydroxylase* mRNA expression and a 4-fold increase in serum $1,25(OH)_2D$ concentrations compared with vehicle-treated *Hyp* mice. Serum P_i levels in *Hyp* mice increased significantly after treatment with PD0325901, and the increase was associated with increased renal *Npt2a* mRNA abundance and brush-border membrane Npt2a protein expression. These findings provide evidence that in *Hyp* mice, MAPK signaling is constitutively activated in the kidney and support the hypothesis that the FGF-23-mediated suppression of renal $1,25(OH)_2D$ production and P_i reabsorption depends on activation of MAPK signaling via MEK/ERK1/2. These findings demonstrate the physiologic importance of MAPK signaling in the actions of FGF-23 in regulating renal $1,25(OH)_2D$ and P_i metabolism.

Keywords

FGF-23; XLH; $1,25(OH)_2D$; PHOSPHATE; MAPK

Address correspondence to: Farzana Perwad, MD, Division of Pediatric Nephrology, Department of Pediatrics, University of California San Francisco, 533 Parnassus Avenue, U-585, Box 0748, San Francisco, CA 94143-0748, USA. perwadf@peds.ucsf.edu.

Disclosures

All the authors state that they have no conflicts of interest.

Introduction

Fibroblast growth factor 23 (FGF-23) is increased in the circulation of patients with the hypophosphatemic syndromes autosomal dominant hypophosphatemic rickets (ADHR), autosomal recessive hypophosphatemic rickets (ARHR), X-linked hypophosphatemia (XLH), and tumor-induced osteomalacia (TIO).[1–4] These syndromes share common clinical features, including hypophosphatemia owing to renal phosphate (P_i) wasting, low or inappropriately normal serum 1,25-dihydroxyvitamin D_3 [1,25$(OH)_2$D] concentrations, and rickets or osteomalacia. In humans, XLH is caused by loss-of-function mutations in the *phosphate-regulating gene with homologies to endopeptidases on the X chromosome* (*PHEX*) gene.[5–8] In the *Hyp* mouse, the murine homologue of XLH, the disorder is caused by a large 3′ deletion mutation in the homologous gene *phex*.[9,10] Loss of *PHEX*/*phex* function in XLH and *Hyp* mice results in increased production by bone and thereby excess circulating concentrations of FGF-23.[11]

FGF-23 acts on the kidney to inhibit the activity and expression of sodium-dependent P_i (Na/P_i) cotransporter Npt2a, thereby inhibiting renal P_i reabsorption and inducing hypophosphatemia.[12–14] FGF-23 also suppresses the renal production of 1,25$(OH)_2$D by inhibiting 1α-hydroxylase and stimulating 24-hydroxylase expression,[13,14] the enzymes responsible for the synthesis and degradation of 1,25$(OH)_2$D, respectively. In XLH and *Hyp* mice, serum 1,25$(OH)_2$D concentrations are inappropriately normal for the degree of hypophosphatemia present. Double-mutant mice bearing the *phex* mutation and *fgf23* gene ablation show reversal of the *Hyp* phenotype, providing direct evidence that FGF-23 is critical to the pathogenesis of XLH.[11,15]

FGF-23 binds to FGF receptor (FGFR) isoforms 1c, 3c, and 4, and this binding requires an obligatory cofactor, klotho, to initiate signal transduction via activation of the mitogen-activated protein kinase (MAPK) signaling pathway.[16,17] The MAPK signaling pathway consists of four major cascades: extracellular signal-regulated kinases (ERK1/2), p38MAPK, c-Jun NH_2-terminal kinases (JNK), and extracellular signal-regulated kinase 5 (ERK5). Activation of MAPK signaling upregulates the expression of *early growth response 1* (*egr1*) gene, which is an immediate-early response gene encoding a zinc finger transcription factor.[18,19] In cultured opossum kidney proximal tubule epithelial cells, FGF-23 activates ERK1/2 and p38 phosphorylation to inhibit Na/P_i cotransport, and this effect is blocked by prior treatment of cells with selective MAP kinase kinase (MEK) and p38 inhibitors, respectively.[20] We showed previously in mouse renal proximal tubule epithelial cells that FGF-23 suppresses *1α-hydroxylase* mRNA expression, and this effect depends on activation of MEK/ERK1/2 signaling; activation of p38 MAPK was not detected in those experiments.[14] Similar to findings in cultured cells, administration of FGF-23 in normal mice activates MEK/ERK1/2 signaling and upregulates *egr1* in the kidney.[16,21] However, it is not known whether the suppressive effects of FGF-23 on renal P_i and vitamin D metabolism in vivo depend on activation of MAPK signaling.

In this study we examined the MAPK signaling pathway in *Hyp* mice. First, we hypothesized that MEK/ERK1/2 signaling is constitutively active in the kidney in *Hyp* mice owing to the increased circulating FGF-23 concentrations. Then we tested the hypothesis

that in *Hyp* mice the FGF-23-induced suppression of renal P_i and $1,25(OH)_2D$ metabolism depends on constitutive activation of MEK/ERK1/2 signaling.

Materials and Methods

Animals

We studied male C57BL/6J *Hyp* mice and their wild-type littermates, 70 to 90 days of age, purchased from Jackson Laboratories (Bar Harbor, ME, USA). All mice were fed a diet containing 0.6% phosphorus and 1% calcium for 4 days before experiments. To determine the effect of FGF-23 on the MAPK signaling pathway, wild-type mice were injected intravenously or intraperitoneally with recombinant human FGF-23(R176Q) (Genzyme Corporation, Framingham, MA, USA), 150 ng/g of body weight and euthanized either 10 or 60 minutes later. Recombinant FGF-23(R176Q) contains a mutation that is identical to that in patients with ADHR, is resistant to proteolytic processing,[22] and has enhanced biologic potency in vivo and in vitro compared with native FGF-23.[23,24] Animals were anesthetized with ketamine, and blood was obtained for determination of serum calcium (Ca), P_i, $1,25(OH)_2D$, and intact parathyroid hormone (iPTH) concentrations. The kidneys were removed and frozen for subsequent preparation of total RNA and protein. To determine the effect of blockade of MAPK signaling on renal P_i and vitamin D metabolism, wild-type and *Hyp* mice were administered the MEK inhibitor PD0325901 (12.5 mg/kg per dose) or vehicle via oral gavage at 24-hour intervals for 4 days. On day 4, the mice were euthanized, and their blood was collected 2 hours after administration of the MEK inhibitor. The kidneys were removed as described earlier, and the femurs were removed for extraction of total RNA. PD0325901 is a second-generation benzhydroxamate ester that selectively inhibits the activity of MEK in mice and humans. PD0325901 blocks phosphorylation of ERK1/2, the activator kinase immediately downstream of MEK, without blocking phosphorylation of p38, JNK, or ERK5.[25–27] PD0325901 has improved oral bioavailability and aqueous solubility over its parent compound, CI-1040.[25–29] All procedures were approved by the Committee on Animal Research at the University of California San Francisco.

Serum biochemistry

Serum phosphorus and calcium concentrations were determined using kits from Stanbio Laboratories (San Antonio, TX, USA). Serum $1,25(OH)_2D$ concentrations were determined using an enzyme immunoassay (EIA) kit from Immunodiagnostic Systems, Inc. (Scottsdale, AZ, USA). Serum iPTH concentrations were determined using an EIA kit from Immutopics International (San Clemente, CA, USA).

Real-time PCR

Total RNA was isolated from kidney and bone using TRIzol reagent (Invitrogen, Carlsbad, CA, USA). cDNA was synthesized using 1X PCR buffer, 7.5 mM $MgCl_2$, 1 mM deoxynucleoside triphosphate (dNTP), 5 M random primers, and 2.5 U/L MMLVRT enzyme at the following temperatures: 25°C for 10 minutes, 48°C for 40 minutes, and 95°C for 5 minutes. Mouse *egr1*, *fgf23*, and *gapdh* probes and primers were purchased from Roche (Indianapolis, IN, USA). The *1α-hydroxylase*, *24-hydroxylase*, *β-glucuronidase* (*Gus*), *Npt2a*, and *Npt2c* probes and primers were custom designed and purchased from

Integrated DNA Technologies (Coralville, IA, USA). The sequences are as follows: *Gus*: forward primer, 5′-CTC ATC TGG AAT TTC GCC GA-3′; probe, 5′6-FAM CGA ACC AGT CAC CGC TGA GAG TAA TCG TAMRA-3′; reverse primer, 5′-GGC GAG TGA AGA TCC CCT TC-3′; *1α-hydroxylase*: forward primer, 5′-CCT CTG CCG AGA CTG GGA-3′; probe, 5′6-FAM TGT TTG CCT TTG CCC AGA GGC AC TAMRA-3′; reverse primer, 5′-TCC CGA AAA AGG AAG TGG GT-3′; and *24-hydroxylase*: forward primer, 5′-TAC GCT GCT GTC ACG GAG C-3′; probe, 5′6-FAM CAG TGG AGA CGA CCG CAA ACA GCT T TAMRA-3′; reverse primer 5′-TCT GGA TTT CCC GGA GAA GTC-3′. The *Npt2a* and *Npt2c* probe and primer sequences were published previously.[30,31] The mRNA abundance of the gene of interest, expressed relative to that of *Gus* or *Gapdh* mRNA, was quantitated by real-time polymerase chain reaction (PCR) using the ABI 7900 HT Sequence Detection System (Applied BioSystems, Inc., Foster City, CA, USA), as described previously.[14] Two hundred and fifty nanograms of template cDNA was used per PCR reaction, and the samples were amplified with an initial melt at 95°C for 10 minutes followed by 45 cycles at 95°C for 15 seconds and at 60°C for 1 minute. The threshold cycle (C_t) at which a statistically significant increase in signal above background fluorescence was determined and the C_t values for the gene of interest were normalized to C_t values for *Gus* or *Gapdh*. A passive reference dye, ROX, was used to normalize for variations in volume or dye concentration between sample wells.

Western blot analysis

Activation of MAPK signaling in the kidney was determined by detection of phosphorylated ERK (pERK1/2) and phosphorylated p38 protein. Mouse kidney total protein (25 μg) was fractionated on 8% polyacrylamide gels in the presence of SDS and transferred to a polyvinylidene fluoride (PVDF) membrane using a semidry transfer apparatus. The membranes were probed with rabbit anti-phospho-ERK1/2 monoclonal antibody (Cell Signaling Technology, Danvers, MA, USA) or rabbit anti-phospho-p38 monoclonal antibody (Cell Signaling Technology) using the SNAP i.d. immunodetection system (Millipore, Billerica, MA, USA) and visualized by chemiluminescence (Supersignal West Dura, Pierce Biotechnology, Rockford, IL, USA). Protein loading was determined using a mouse anti-ERK 2 monoclonal antibody (Santa Cruz Biotechnology, Inc., Santa Cruz, CA, USA) and rabbit anti-p38 polyclonal antibody (Cell Signaling Technology). For detection of Npt2a protein, renal brush-border membrane vesicles (BBMVs) were prepared as described previously.[32] From these membranes, protein was prepared for Western blot analysis, and 25 μg of protein was transferred to PVDF membranes as described earlier. The membranes were probed with a rabbit anti-Npt2a polyclonal antibody (Alpha Diagnostic International, Inc., San Antonio, TX, USA). Protein loading was determined using a rabbit anti-β-actin polyclonal antibody (Cell Signaling Technology). For detection of 1α-hydroxylase protein, renal mitochondrial protein was isolated by the method of Vieth and Fraser, as described previously.[33] Then 35 μg of protein was transferred to PVDF membranes as described earlier, and the membranes were probed with a rabbit anti-1α-hydroxylase polyclonal antibody (Santa Cruz Biotechnology). Protein loading was determined using a rabbit anti-β-actin polyclonal antibody (Cell Signaling Technology).

Statistical analysis

Data are expressed as means ± SEM. The significance of differences between vehicle and treatment groups was analyzed by Mann-Whitney rank-sum test or between multiple groups by two-way analysis of variance (ANOVA) using Sigma Stat statistical software (Jandel Scientific, San Rafael, CA, USA). Post hoc testing was performed using the Student-Newman-Keuls test. A p value of less than .05 was considered statistically significant.

Results

Activation of MAPK signaling in wild-type and *Hyp* mice

To examine the acute effect of FGF-23 on MAPK signaling in the kidney in vivo, we administered a single dose of FGF-23(R176Q) (150 ng/g of body weight) to wild-type mice. Activation of MAPK signaling was determined by detection of ERK1/2 phosphorylation on Western blot and increased *egr1* mRNA expression by real-time PCR. FGF-23 induced an increase in the renal abundance of pERK1/ 2 protein as early as 10 minutes after injection compared with mice injected with vehicle, and this effect persisted at 60 minutes after injection (Fig. 1*A*). ERK1/2 phosphorylation was accompanied by a 5-fold increase (p <.05) in the renal abundance of *egr1* mRNA at 60 minutes after injection (Fig. 1*B*).

In *Hyp* mice, circulating FGF-23 is greatly increased.[11,34] To determine whether MAPK signaling is activated under normal conditions, we measured the abundance of pERK1/2 and p38 proteins and *egr1* mRNA in kidneys from *Hyp* and wild-type mice fed a constant-P_i diet. The abundance of pERK1/2 (Fig. 2*A*) and p38 (data not shown) proteins in *Hyp* mice did not differ from that in wild-type mice at baseline (Fig. 2*A*). However, the abundance of *egr1* mRNA in *Hyp* mice was approximately 2-fold higher in *Hyp* than in wild-type mice (p <.05), as determined by real-time PCR (Fig. 2*B*).

To induce blockade of MEK/ERK1/2 signaling and to determine whether the increased *egr1* gene expression in *Hyp* mice was due to activation of the MEK/ERK1/2 signaling cascade, we treated wild-type and *Hyp* mice with the highly selective MEK inhibitor PD0325901. Treatment with PD0325901 abolished renal ERK1/2 phosphorylation and suppressed *egr1* gene expression by 13-fold in wild-type mice and by 16-fold in *Hyp* mice (p <.05; Fig. 2*A*, *B*).

Effects of MEK/ERK1/2 signaling blockade on renal 1,25$(OH)_2$D metabolism

To determine the effect of blockade of MEK/ERK1/2 signaling on 1,25$(OH)_2$D metabolism, we treated wild-type and *Hyp* mice with PD0325901 or vehicle and measured the renal abundance of *1α-hydroxylase* mRNA by real-time PCR (Fig. 3*A*). Under baseline conditions (vehicle), *1α-hydroxylase* mRNA abundance in *Hyp* mice was 3-fold higher than that in wild-type mice, consistent with previous reports.[35] After treatment with PD0325901, *1α-hydroxylase* mRNA did not change significantly in wild-type mice but increased by 8-fold in *Hyp* mice (p <.05) compared with mice treated with vehicle; the posttreatment values remained higher in *Hyp* than in wild-type mice (p <.05). We then determined whether the increase in *1α-hydroxylase* mRNA expression in PD0325901-treated *Hyp* mice was associated with changes in renal mitochondrial 1α-hydroxylase protein. Western blot

analysis showed that treatment with PD0325901 induced an increase in renal mitochondrial 1α-hydroxylase protein compared with the vehicle-treated group (Fig. 3*B*). The renal abundance of *24-hydroxylase* mRNA did not differ between wild-type and *Hyp* mice at baseline and did not change significantly after treatment with PD0325901 (Fig. 3*C*). At baseline, serum concentrations of $1,25(OH)_2D$ were not significantly different between wild-type and *Hyp* mice, consistent with prior reports[35] (Fig. 4). After treatment with PD0325901, serum concentrations of $1,25(OH)_2D$ increased by 1.5-fold in wild-type mice (93 ± 18 versus 141 ± 20 pg/mL, mean ± SEM, p =NS) and by 4-fold in *Hyp* mice (89 ± 21 versus 350 ± 41 pg/mL, p <.05). Serum concentrations of $1,25(OH)_2D$ were higher in *Hyp* than in wild-type mice after treatment with PD0325901 (p <.05).

Effects of MEK/ERK1/2 signaling blockade on renal P_i metabolism

At baseline, the mean serum P_i concentration was lower in *Hyp* mice than in wild-type mice, as expected (5.3 ± 0.5 versus 10.5 ± 0.4 mg/dL, p <.05; Fig. 5*A*). After treatment with PD0325901, serum P_i levels increased significantly in both *Hyp* (6.9 ± 0.3 mg/dL) and wild-type mice (12.9 ± 0.5 mg/dL, p <.05 for each group; Fig. 5*A*). At baseline, renal abundance of *Npt2a* mRNA was lower in *Hyp* mice than in wild-type mice (p <.05; Fig. 5*B*). After treatment with PD0325901, *Npt2a* mRNA expression increased significantly in *Hyp* mice (p <.05) but not in wild-type mice. Treatment with PD0325901 also induced an increase in renal brush-border abundance of Npt2a protein in *Hyp* mice (Fig. 5*C*). The renal abundance of *Npt2c* mRNA did not differ between *Hyp* and wild-type mice at baseline and did not change significantly after treatment with PD0325901 (data not shown).

Serum calcium and PTH

The mean serum calcium concentrations did not differ between *Hyp* and wild-type mice at baseline (10 ± 0.5 versus 9.9 ± 0.1 mg/ dL) and did not change significantly in either group after PD0325901 treatment (Fig. 6*A*). At baseline, serum iPTH levels were higher in *Hyp* mice than in wild-type mice, (87 ± 27 versus 7 ± 5 pg/mL, p <.05; Fig. 6*B*). After treatment with PD0325901, serum iPTH levels increased significantly in *Hyp* mice (87 ± 27 versus 135 ± 34 pg/mL, p <.05) and were significantly higher than in wild-type mice treated with PD0325901 (135 ± 34 versus 15 ± 7 pg/mL, p <.05).

Bone *fgf23* mRNA

At baseline, the abundance of *fgf23* mRNA in the femur was 4-fold higher in *Hyp* mice than in wild-type mice (p <.05; Fig. 7), consistent with previous reports,[34,36] and did not increase further after treatment with PD0325901. However, in wild-type mice, PD0325901 induced a 6-fold increase in *fgf23* mRNA abundance (p <.05) compared with the vehicle-treated group.

Discussion

In this study, we demonstrate that FGF-23 acutely activates MAPK signaling via the MEK/ERK1/2 cascade in the kidney in wild-type mice in vivo, confirming previous reports.[16,21] We demonstrate that in *Hyp* mice, MEK/ERK1/2 signaling is constitutively activated in the kidneys compared with wild-type mice. Treatment of *Hyp* mice with the MEK inhibitor

PD0325901 suppresses renal MEK/ERK1/2 signal activation, thereby inducing upregulation of renal *1α-hydroxylase* mRNA expression, increased serum $1,25(OH)_2D$ concentrations, increased renal *Npt2a* expression, and partial correction of hypophosphatemia. Thus these data support the hypothesis that in *Hyp* mice, the FGF-23-mediated suppression of renal $1,25(OH)_2D$ production and P_i reabsorption depends on activation of MAPK signaling via MEK/ ERK1/2.

We sought to determine the importance of MAPK signaling in the renal actions of FGF-23 in vivo. First, we demonstrated that FGF-23 acutely activates MEK/ERK1/2 signaling in the kidney in normal mice. A single injection of recombinant FGF-23 in wild-type mice induced phosphorylation of pERK1/2 as early as 10 minutes and increased *egr1* mRNA expression at 1 hour after injection, consistent with previously published data.[16,21] We then evaluated the activity of MAPK signaling in the kidneys of *Hyp* mice, in which circulating FGF-23 is greatly increased as a result of its increased gene expression in bone.[34,36] We found that at baseline, renal *egr1* mRNA abundance was significantly higher in *Hyp* than in wild-type mice. We then administered the MEK inhibitor PD0325901, which blocks phosphorylation of ERK1/2 in both humans and mice. Treatment with PD0325901 greatly suppressed pERK1/2 and *egr1* mRNA expression in both wild-type and *Hyp* mice. Although *egr1* expression can be upregulated by the other MAPK signaling cascades as well as by MEK/ ERK1/2, our finding that PD0325901 was sufficient to suppress *egr1* mRNA by more than 90% suggests that its increased expression in *Hyp* mice depends on MEK/ERK1/2 signaling. These results provide evidence that in *Hyp* mice, the increase in circulating FGF-23 induces constitutive activation of MEK/ERK1/2 signaling in the kidney.

FGF-23 suppresses renal $1,25(OH)_2D$ production by down-regulating renal *1α-hydroxylase* gene expression and upregulating *24-hydroxylase* gene expression.[13,14] We hypothesized that in *Hyp* mice, the low or inappropriately normal serum concentrations of $1,25(OH)_2D$ reflect suppression of its production by excess FGF-23, and this suppression depends on activation of MAPK signaling. We observed that at baseline in *Hyp* mice, serum $1,25(OH)_2D$ concentrations were inappropriately normal for the degree of hypophosphatemia, similar to prior data.[37] Baseline renal *1α-hydroxylase* mRNA expression was higher in *Hyp* than in wild-type mice, whereas *24-hydroxylase* mRNA was not different from that in wild-type mice, as we reported previously.[35] Treatment of *Hyp* mice with PD0325901 induced a 4-fold increase in serum $1,25(OH)_2D$ concentrations, and the increase was associated with a several-fold increase in renal *1α-hydroxylase* mRNA expression but no significant change in *24-hydroxylase* mRNA. These results provide evidence that in *Hyp* mice, blockade of FGF-23-dependent MEK/ERK1/2 activation induced a substantial increase in renal production of $1,25(OH)_2D$. Although we did not measure $1,25(OH)_2D$ production directly in this study, we showed previously in *Hyp* and wild-type mice that increases in renal *1α-hydroxylase* mRNA induced by manipulating dietary phosphorus correlated highly significantly with increases in renal mitochondria 1α-hydroxylase enzyme activity.[35] Moreover, in this study, we show in *Hyp* mice that PD0325901 induced an increase in renal mitochondria 1α-hydroxylase protein abundance by Western blot analysis. It is possible that a reduction in 24-hydroxylase activity, induced by PD0325901, contributed to an increase in $1,25(OH)_2D$ production in *Hyp* mice, although

we observed no significant changes in *24-hydroxylase* mRNA with PD901 treatment in either strain of mice. However, Tenenhouse and colleagues showed in phosphate-deprived *Hyp* mice that when renal *24-hydroxylase* mRNA and enzyme activity were suppressed to normal values by growth-hormone treatment, serum $1,25(OH)_2D$ concentrations did not increase and concluded that changes in *24-hydroxylase* activity did not contribute to the inappropriately low serum $1,25(OH)_2D$ concentrations in *Hyp* mice.[38] Thus it remains to be determined whether and to what extent an FGF-23-dependent increase in basal *cyp24* gene expression in *Hyp* mice contributes to the aberrant regulation of their serum $1,25(OH)_2D$ concentrations.

FGF-23 suppresses renal P_i reabsorption by downregulating expression of Npt2a in the proximal tubule.[12,39] We hypothesized that in *Hyp* mice, the FGF-23-induced suppression of renal P_i reabsorption is mediated by activation of MAPK signaling. As expected, we found that at baseline, serum P_i concentrations were lower in *Hyp* mice than in wild-type mice. Treatment of *Hyp* mice with PD0325901 induced a significant increase in serum P_i concentrations, although the mean value remained lower than that in wild-type mice. The increase in serum P_i concentration in *Hyp* mice was associated with an increase in renal *Npt2a* mRNA expression and in renal brush border membrane Npt2a protein abundance. In *Hyp* mice, renal expression of the sodium-dependent P_i cotransporter Npt2c also has been shown to be decreased.[40] However, in this study, *Npt2c* mRNA expression at baseline was not significantly lower in *Hyp* than in wild-type mice, and the expression did not change after treatment with PD0325901 in either group of animals. These findings demonstrate that in *Hyp* mice, blockade of the FGF-23-mediated MEK/ERK1/2 signaling upregulates renal *Npt2a* mRNA and protein expression and partially corrects the hypophosphatemia. The failure of MEK/ERK1/2 blockade to fully correct the hypophosphatemia in *Hyp* mice may reflect constitutive activation of alternate signaling pathways or the increase in serum iPTH concentration observed when PD0325901 was administered. Although in vitro studies showed that FGF-23-induced inhibition of P_i transport in part depends on activation of p38 MAPK,[20] we did not detect activation of the p38 MAPK signaling cascade in *Hyp* mice.

In this study, baseline serum iPTH concentrations were higher in *Hyp* mice than in wild-type mice, consistent with prior reports.[41] After treatment with PD0325901, mean iPTH levels increased significantly in *Hyp* mice. This increase may be a physiologic response to the increased serum P_i concentrations induced by treatment with PD0325901. Alternatively, FGF-23 administration in rats has been shown to suppress iPTH synthesis, and such suppression depends on activation of MAPK signaling in the parathyroid gland.[42] Thus in this study the increase in iPTH concentrations induced by PD0325901 may reflect partial blockade of FGF-23-mediated suppression of iPTH synthesis. Further experiments are required to investigate the role of MAPK signaling in the regulation of iPTH by FGF-23 in *Hyp* mice. Serum calcium concentrations were not significantly different between wild-type and *Hyp* mice at baseline, and the levels did not change significantly after treatment with PD0325901.

In *Hyp* mice[34,36] and in normal mice fed a high-P_i diet,[33] the increased serum FGF-23 concentrations observed are associated with increased *fgf23* mRNA expression in bone, suggesting that circulating FGF-23 reflects its production by bone. In this study, we

confirmed that *fgf23* mRNA expression in bone is higher in *Hyp* than in wild-type mice at baseline and observed that after treatment with PD0325901, *fgf23* mRNA increased, if not significantly, in both strains. Although we did not measure serum FGF-23 directly in this study, the data suggest that circulating FGF-23 concentrations were not suppressed by systemic inhibition of MEK/ERK1/2 signaling.

In this study, we characterized the effects of FGF-23 on only the MEK/ERK1/2 and p38 signaling pathways. Recent data suggest that other pathways may be involved in mediating the effects of FGF-23 on renal $1,25(OH)_2D$ metabolism, at least in vitro. In primary renal proximal tubule cells, treatment with FGF-23 and klotho induced phosphorylation of protein kinase B (AKT) of the phosphotidylinositol 3-kinase (PI3K) signaling pathway and the ERK1/2, p38, and JNK of the MAPK signaling pathway and suppressed the expression of 1α-hydroxylase protein.[43] However, such suppression was not fully reversed by selective inhibition of the PI3K and ERK1/2 signaling pathways.[43] In our current experiments in *Hyp* mice, inhibition of MEK/ERK1/2 signaling alone completely reversed the suppression of *1α-hydroxylase* gene expression and serum $1,25(OH)_2D$ concentrations. Thus the present data provide evidence that the MEK/ ERK1/2 signaling pathway is the principal pathway involved in the suppression of *1α-hydroxylase* gene expression by FGF-23. Our findings are similar to those observed in *Hyp* mice treated with anti-FGF-23 antibodies, which prevent the binding of FGF-23 to its receptor and cofactor klotho.[44,45] Such treatment reversed the FGF-23-induced suppression of renal *1α-hydroxylase* gene expression and serum$1,25(OH)_2D$ concentrations and completely reversed the hypophosphatemia.[44,45]

In summary, the results of this study provide evidence that in *Hyp* mice, the increased circulating FGF-23 concentrations induce constitutive activation of MAPK signaling via MEK/ ERK1/2 in the kidney, and inhibition of this signaling reverses the FGF-23-dependent suppression of renal *1α-hydroxylase* gene expression, increases serum $1,25(OH)_2D$ concentrations, and partially corrects the hypophosphatemia. These findings demonstrate the physiologic importance of MAPK signaling in the actions of FGF-23 to inhibit renal $1,25(OH)_2D$ production and P_i reabsorption.

Acknowledgments

We thank S Schiavi (Genzyme) for providing the recombinant FGF-23(R176Q) protein used in the study. This work was supported by National Institutes of Health Grant DK-073092, a Normon S Coplon grant (satellite research) (to FP), and the Pediatric Nephrology Innovative Research Fund (to AP).

References

1. Yamazaki Y, Okazaki R, Shibata M, et al. Increased circulatory level of biologically active full-length FGF-23 in patients with hypophosphatemic rickets/osteomalacia. J Clin Endocrinol Metab. 2002; 87:4957–4960. [PubMed: 12414858]
2. Jonsson KB, Zahradnik R, Larsson T, et al. Fibroblast growth factor 23 in oncogenic osteomalacia and X-linked hypophosphatemia. N Engl J Med. 2003; 348:1656–1663. [PubMed: 12711740]
3. Imel EA, Hui SL, Econs MJ. FGF-23 concentrations vary with disease status in autosomal dominant hypophosphatemic rickets. J Bone Miner Res. 2007; 22:520–526. [PubMed: 17227222]
4. Feng JQ, Ward LM, Liu S, et al. Loss of DMP1 causes rickets and osteomalacia and identifies a role for osteocytes in mineral metabolism. Nat Genet. 2006; 38:1310–1315. [PubMed: 17033621]

5. A gene (*PEX*) with homologies with endopeptidases is mutated in patients with X-linked hypophosphatemic rickets. The HYP Consortium. Nat Genet. 1995; 11:130–136. [PubMed: 7550339]
6. Dixon PH, Christie PT, Wooding C, et al. Mutational analysis of PHEX gene in X-linked hypophosphatemia. J Clin Endocrinol Metab. 1998; 83:3615–3623. [PubMed: 9768674]
7. Rowe PS, Oudet CL, Francis F, et al. Distribution of mutations in the PEX gene in families with X-linked hypophosphataemic rickets (HYP). Hum Mol Genet. 1997; 6:539–549. [PubMed: 9097956]
8. Holm IA, Huang X, Kunkel LM. Mutational analysis of the PEX gene in patients with X-linked hypophosphatemic rickets. Am J Hum Genet. 1997; 60:790–797. [PubMed: 9106524]
9. Eicher EM, Southard JL, Scriver CR, Glorieux FH. Hypophosphatemia: mouse model for human familial hypophosphatemic (vitamin D-resistant) rickets. Proc Natl Acad Sci U S A. 1976; 73:4667–4671. [PubMed: 188049]
10. Beck L, Soumounou Y, Martel J, et al. Pex/PEX tissue distribution and evidence for a deletion in the 3′ region of the Pex gene in X-linked hypophosphatemic mice. J Clin Invest. 1997; 99:1200–1209. [PubMed: 9077527]
11. Liu S, Zhou J, Tang W, Jiang X, Rowe DW, Quarles LD. Pathogenic role of Fgf23 in Hyp mice. Am J Physiol Endocrinol Metab. 2006; 291:E38–49. [PubMed: 16449303]
12. Larsson T, Marsell R, Schipani E, et al. Transgenic mice expressing fibroblast growth factor 23 under the control of the alpha1(I) collagen promoter exhibit growth retardation, osteomalacia, and disturbed phosphate homeostasis. Endocrinology. 2004; 145:3087–3094. [PubMed: 14988389]
13. Shimada T, Hasegawa H, Yamazaki Y, et al. FGF-23 is a potent regulator of vitamin D metabolism and phosphate homeostasis. J Bone Miner Res. 2004; 19:429–435. [PubMed: 15040831]
14. Perwad F, Zhang MY, Tenenhouse HS, Portale AA. Fibroblast growth factor 23 impairs phosphorus and vitamin D metabolism in vivo and suppresses 25-hydroxyvitamin D-1alpha-hydroxylase expression in vitro. Am J Physiol Renal Physiol. 2007; 293:F1577–1583. [PubMed: 17699549]
15. Sitara D, Razzaque MS, Hesse M, et al. Homozygous ablation of fibroblast growth factor-23 results in hyperphosphatemia and impaired skeletogenesis, and reverses hypophosphatemia in Phex-deficient mice. Matrix Biol. 2004; 23:421–432. [PubMed: 15579309]
16. Urakawa I, Yamazaki Y, Shimada T, et al. Klotho converts canonical FGF receptor into a specific receptor for FGF23. Nature. 2006; 444:770–774. [PubMed: 17086194]
17. Kurosu H, Ogawa Y, Miyoshi M, et al. Regulation of fibroblast growth factor-23 signaling by klotho. J Biol Chem. 2006; 281:6120–6123. [PubMed: 16436388]
18. Lim CP, Jain N, Cao X. Stress-induced immediate-early gene, egr-1, involves activation of p38/JNK1. Oncogene. 1998; 16:2915–2926. [PubMed: 9671412]
19. Guha M, O'Connell MA, Pawlinski R, et al. Lipopolysaccharide activation of the MEK-ERK1/2 pathway in human monocytic cells mediates tissue factor and tumor necrosis factor alpha expression by inducing Elk-1 phosphorylation and Egr-1 expression. Blood. 2001; 98:1429–1439. [PubMed: 11520792]
20. Yamashita T, Konishi M, Miyake A, Inui K, Itoh N. Fibroblast growth factor (FGF)-23 inhibits renal phosphate reabsorption by activation of the mitogen-activated protein kinase pathway. J Biol Chem. 2002; 277:28265–28270. [PubMed: 12032146]
21. Farrow EG, Davis SI, Summers LJ, White KE. Initial FGF23-mediated signaling occurs in the distal convoluted tubule. J Am Soc Nephrol. 2009; 20:955–960. [PubMed: 19357251]
22. White KE, Carn G, Lorenz-Depiereux B, Benet-Pages A, Strom TM, Econs MJ. Autosomal-dominant hypophosphatemic rickets (ADHR) mutations stabilize FGF-23. Kidney Int. 2001; 60:2079–2086. [PubMed: 11737582]
23. Shimada T, Muto T, Urakawa I, et al. Mutant FGF-23 responsible for autosomal dominant hypophosphatemic rickets is resistant to proteolytic cleavage and causes hypophosphatemia in vivo. Endocrinology. 2002; 143:3179–3182. [PubMed: 12130585]
24. Bai XY, Miao D, Goltzman D, Karaplis AC. The autosomal dominant hypophosphatemic rickets R176Q mutation in fibroblast growth factor 23 resists proteolytic cleavage and enhances in vivo biological potency. J Biol Chem. 2003; 278:9843–9849. [PubMed: 12519781]

25. Cohen P. Protein kinases–the major drug targets of the twenty-first century? Nat Rev Drug Discov. 2002; 1:309–315. [PubMed: 12120282]
26. Brown AP, Carlson TC, Loi CM, Graziano MJ. Pharmacodynamic and toxicokinetic evaluation of the novel MEK inhibitor, PD0325901, in the rat following oral and intravenous administration. Cancer Che-mother Pharmacol. 2007; 59:671–679.
27. Bain J, Plater L, Elliott M, et al. The selectivity of protein kinase inhibitors: a further update. Biochem J. 2007; 408:297–315. [PubMed: 17850214]
28. Sebolt-Leopold JS. Advances in the development of cancer therapeutics directed against the RAS-mitogen-activated protein kinase pathway. Clin Cancer Res. 2008; 14:3651–3656. [PubMed: 18559577]
29. Barrett SD, Bridges AJ, Dudley DT, et al. The discovery of the benzhydroxamate MEK inhibitors CI-1040 and PD 0325901. Bioorg Med Chem Lett. 2008; 18:6501–6504. [PubMed: 18952427]
30. Yu X, Sabbagh Y, Davis SI, Demay MB, White KE. Genetic dissection of phosphate- and vitamin D-mediated regulation of circulating Fgf23 concentrations. Bone. 2005; 36:971–977. [PubMed: 15869926]
31. Madjdpour C, Bacic D, Kaissling B, Murer H, Biber J. Segment-specific expression of sodium-phosphate cotransporters NaPi-IIa and -IIc and interacting proteins in mouse renal proximal tubules. Pflugers Arch. 2004; 448:402–410. [PubMed: 15007650]
32. Biber J, Stieger B, Stange G, Murer H. Isolation of renal proximal tubular brush-border membranes. Nat Protoc. 2007; 2:1356–1359. [PubMed: 17545973]
33. Zhang MY, Wang X, Wang JT, et al. Dietary phosphorus transcriptionally regulates 25-hydroxyvitamin D-1alpha-hydroxylase gene expression in the proximal renal tubule. Endocrinology. 2002; 143:587–595. [PubMed: 11796514]
34. Perwad F, Azam N, Zhang MY, Yamashita T, Tenenhouse HS, Portale AA. Dietary and serum phosphorus regulate fibroblast growth factor 23 expression and 1,25-dihydroxyvitamin D metabolism in mice. Endocrinology. 2005; 146:5358–5364. [PubMed: 16123154]
35. Azam N, Zhang MY, Wang X, Tenenhouse HS, Portale AA. Disordered regulation of renal 25-hydroxyvitamin D-1alpha-hydroxylase gene expression by phosphorus in X-linked hypophosphatemic (hyp) mice. Endocrinology. 2003; 144:3463–3468. [PubMed: 12865326]
36. Liu S, Guo R, Simpson LG, Xiao ZS, Burnham CE, Quarles LD. Regulation of fibroblastic growth factor 23 expression but not degradation by PHEX. J Biol Chem. 2003; 278:37419–37426. [PubMed: 12874285]
37. Tenenhouse HS, Jones G. Abnormal regulation of renal vitamin D catabolism by dietary phosphate in murine X-linked hypophosphatemic rickets. J Clin Invest. 1990; 85:1450–1455. [PubMed: 2332500]
38. Roy S, Martel J, Tenenhouse HS. Growth hormone normalizes renal 1,25 dihydroxyvitamin D3-24-hydroxylase gene expression but not Na+-phosphate cotransporter (Npt2) mRNA in phosphate-deprived Hyp mice. J Bone Miner Res. 1997; 12:1672–1680. [PubMed: 9333128]
39. Shimada T, Urakawa I, Yamazaki Y, et al. FGF-23 transgenic mice demonstrate hypophosphatemic rickets with reduced expression of sodium phosphate cotransporter type IIa. Biochem Biophys Res Commun. 2004; 314:409–414. [PubMed: 14733920]
40. Tenenhouse HS, Martel J, Gauthier C, Segawa H, Miyamoto K. Differential effects of Npt2a gene ablation and X-linked Hyp mutation on renal expression of Npt2c. Am J Physiol Renal Physiol. 2003; 285:F1271–1278. [PubMed: 12952859]
41. Kiebzak GM, Roos BA, Meyer RA Jr. Secondary hyperparathyroidism in X-linked hypophosphatemic mice. Endocrinology. 1982; 111:650–652. [PubMed: 6807667]
42. Ben-Dov IZ, Galitzer H, Lavi-Moshayoff V, et al. The parathyroid is a target organ for FGF23 in rats. J Clin Invest. 2007; 117:4003–4008. [PubMed: 17992255]
43. Medici D, Razzaque MS, Deluca S, et al. FGF-23-Klotho signaling stimulates proliferation and prevents vitamin D-induced apoptosis. J Cell Biol. 2008; 182:459–465. [PubMed: 18678710]
44. Yamazaki Y, Tamada T, Kasai N, et al. Anti-FGF23 neutralizing antibodies show the physiological role and structural features of FGF23. J Bone Miner Res. 2008; 23:1509–1518. [PubMed: 18442315]

45. Aono Y, Yamazaki Y, Yasutake J, et al. Therapeutic effects of anti-FGF23 antibodies in hypophosphatemic rickets/osteomalacia. J Bone Miner Res. 2009; 24:1879–1888. [PubMed: 19419316]

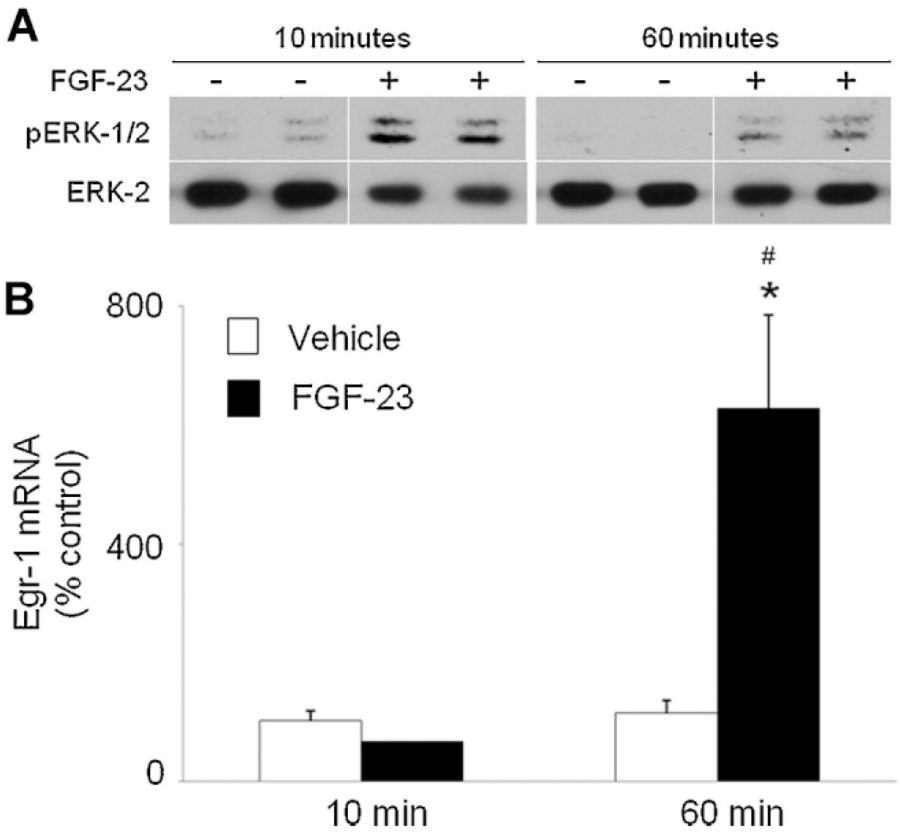

Fig. 1.

Effect of FGF-23 on renal MEK/ERK1/2 signaling in wild-type mice. Mice were injected with FGF-23 or vehicle and euthanized 10 and 60 minutes later. (*A*) Whole-kidney tissue protein extracts were probed with rabbit anti-phospho-ERK1/2 antibodies (*top panel*). Protein loading was determined using total ERK2 protein (*bottom panel*). (*B*). *Egr1* mRNA abundance was quantitated by real-time PCR, normalized to that of *Gus* mRNA, and expressed as a percent relative to vehicle. Bars depict mean ± SEM (n = 4 to 6 mice/group). $^{*}p < .05$ compared with the vehicle group.

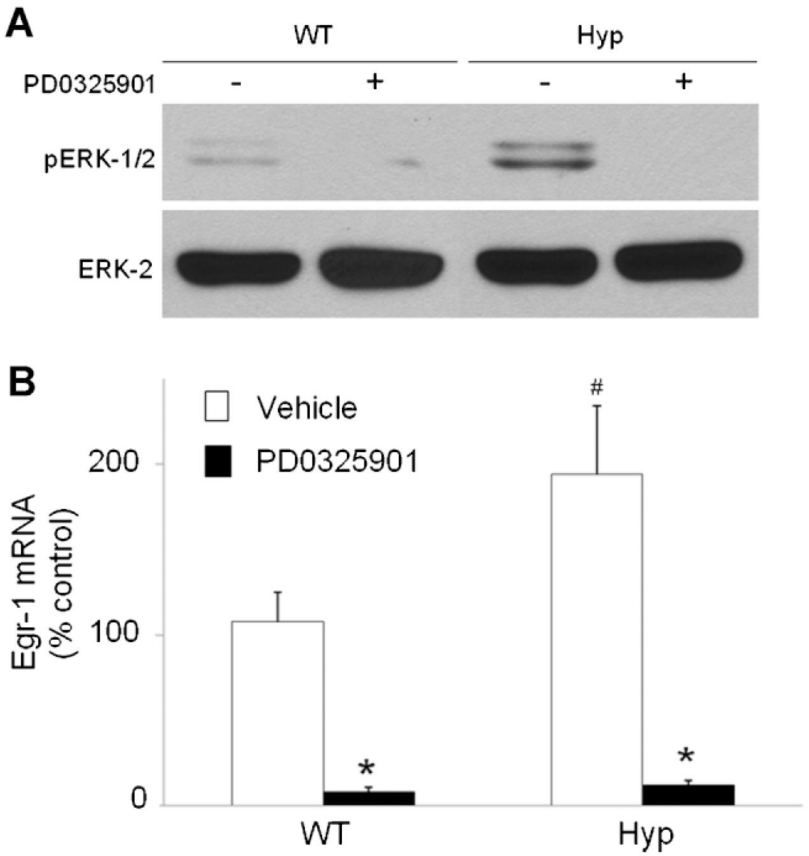

Fig. 2.

Effect of PD0325901 on renal MEK/ERK1/2 signaling in wild-type and *Hyp* mice. Mice were administered PD0325901 or vehicle for 4 days. (*A*) Whole-kidney tissue protein extracts were probed with rabbit anti-phospho-ERK1/2 antibodies. (*B*) *Egr1* mRNA abundance, normalized to that of *Gus* mRNA, is expressed as a percent relative to vehicle-treated wild-type mice. Bars depict mean ± SEM (n =7 to 8 mice/group). $^{\#}p$ <.05 compared with wild-type mice treated with vehicle. $^{*}p$ <.05 compared with vehicle-treated mice within each mouse strain.

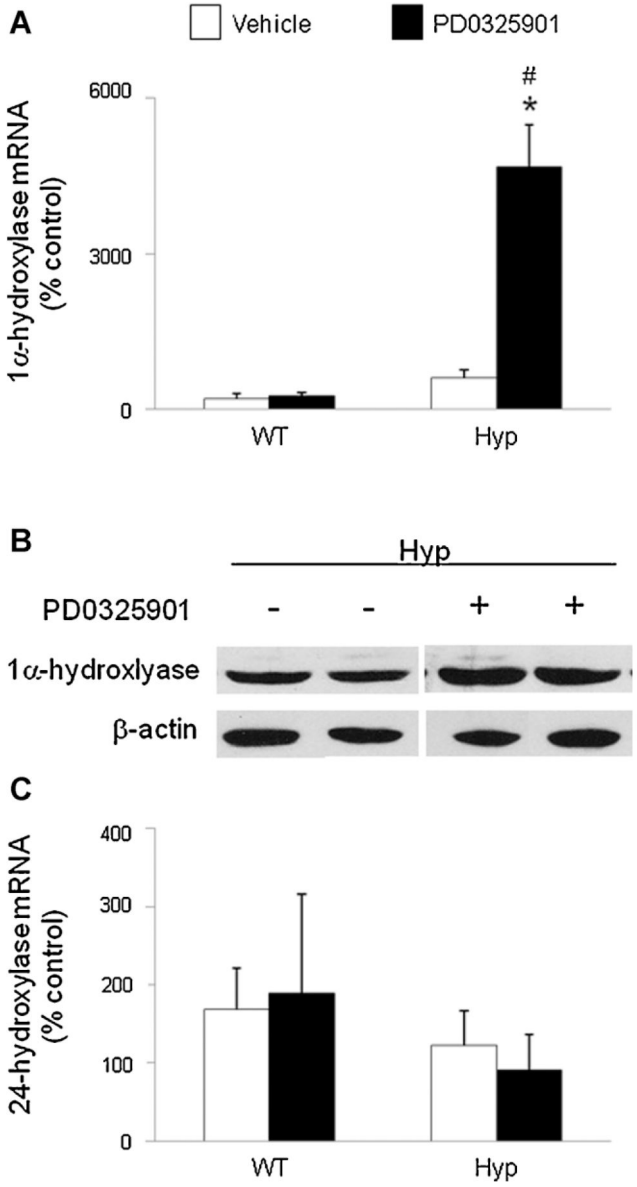

Fig. 3.

Effects of MEK inhibition by PD0325901 on 1,25$(OH)_2$D metabolism in wild-type and *Hyp* mice. Mice were administered PD0325901 or vehicle for 4 days. (*A*) Renal *1α-hydroxylase* mRNA abundance was quantitated by real-time PCR, normalized to that of *Gus* mRNA, and expressed as a percent relative to vehicle-treated wild-type mice. (*B*) Renal mitochondrial 1α-hydroxylase protein abundance in *Hyp* mice determined by a Western blot analysis. Protein loading was determined using β-actin. The immunoblot represents data from 2 mice/group. (*C*) Renal *24-hydroxylase* mRNA abundance was quantitated as above. Bars depict mean ± SEM (n =7 to 12 mice/group). $^{\#}p$ <.05 compared with wild-type mice within each treatment group. $^{*}p$ <.05 compared with vehicle-treated mice within each mouse strain.

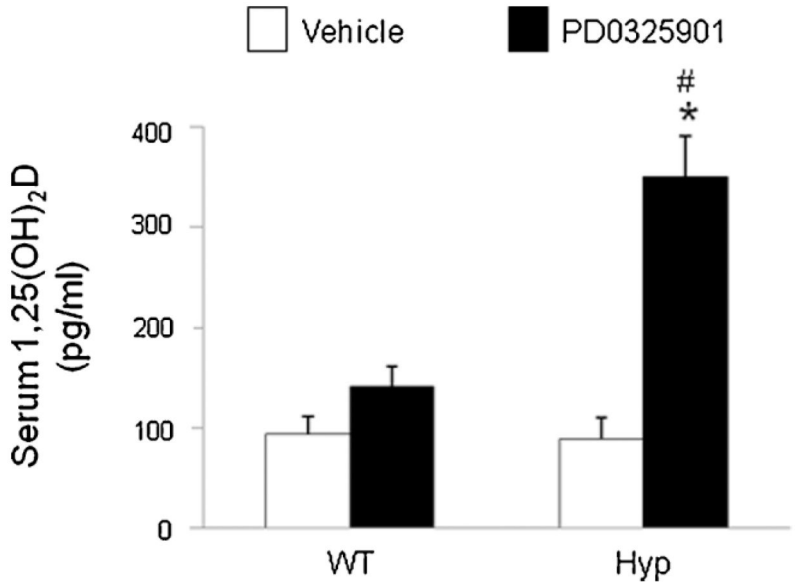

Fig. 4.

Effects of MEK inhibition by PD0325901 on serum $1,25(OH)_2D$ concentrations in wild-type and *Hyp* mice. Mice were administered PD0325901 or vehicle for 4 days. $^{\#}p < .05$ compared with wild-type mice within each treatment group. $^{*}p < .05$ compared with vehicle-treated mice within each mouse strain.

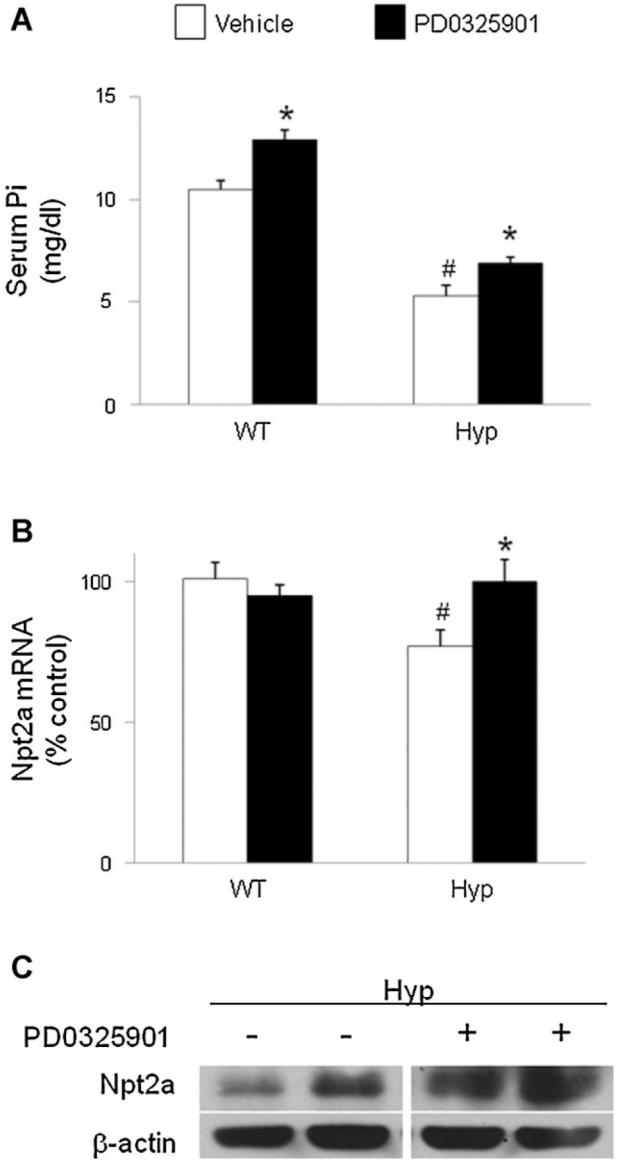

Fig. 5.

Effects of MEK inhibition by PD0325901 on phosphate metabolism in wild-type and *Hyp* mice. Mice were administered PD0325901 or vehicle for 4 days. (*A*) Serum P_i concentrations. (*B*) Renal *Npt2a* mRNA abundance was quantitated by real-time PCR, normalized to that of *Gus* mRNA, and expressed as a percent relative to vehicle-treated wild-type mice. (*C*) Renal brush-border Npt2a protein abundance. Protein loading was determined using β-actin. Bars depict mean ± SEM (n =7 to 12 mice/group) $^{\#}p$ <.05 compared with wild-type mice within each treatment group. $^{*}p$ <.05 compared with vehicle-treated mice within each mouse strain.

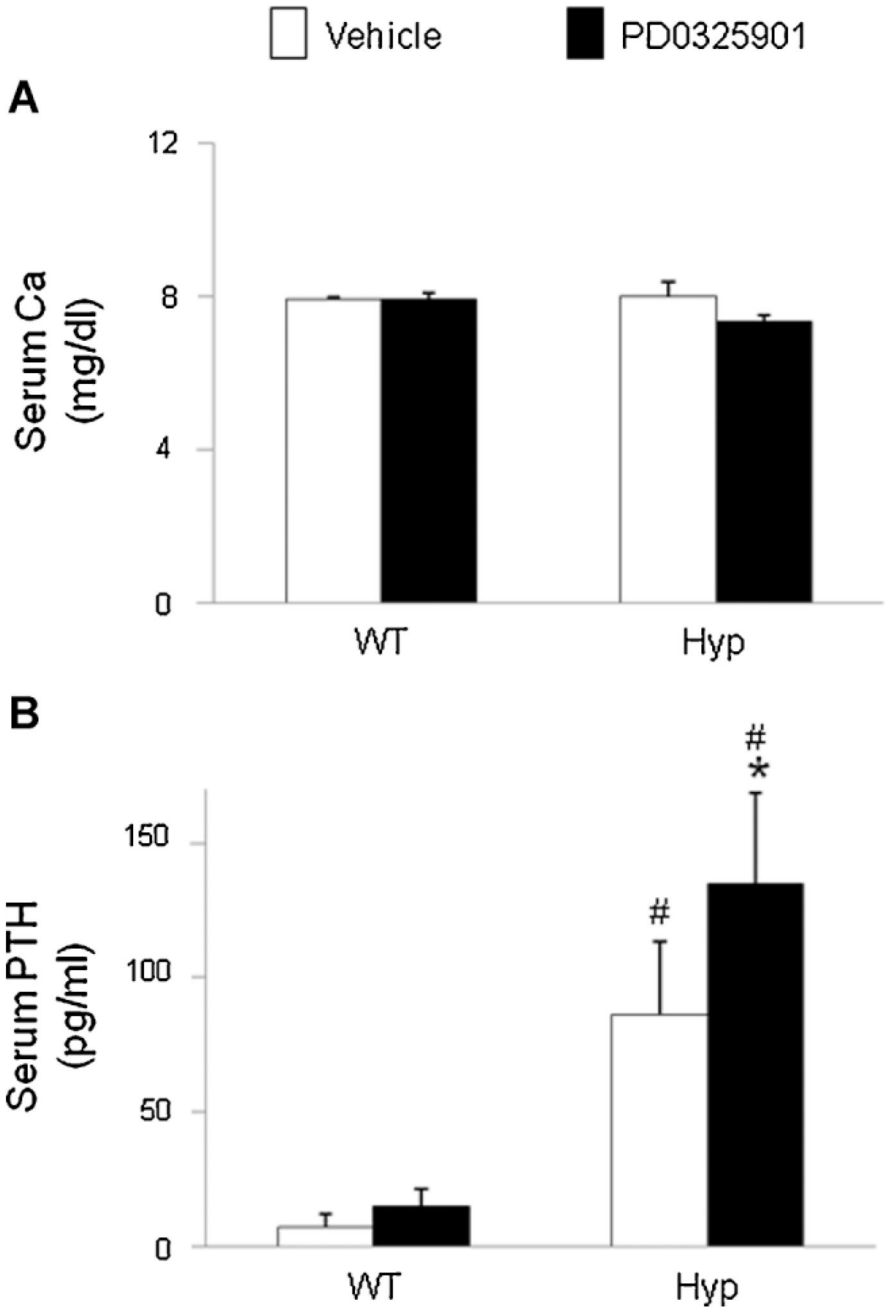

Fig. 6.

Effects of MEK inhibition by PD0325901 on serum calcium and iPTH concentrations in wild-type and *Hyp* mice. Mice were administered PD0325901 or vehicle for 4 days. (*A*) Serum calcium concentrations. (*B*) Serum iPTH concentrations. Bars depict mean ± SEM (n =7 to 12 mice/ group) $^{\#}p$ <.05 compared with wild-type mice within each treatment group. $^{*}p$ <.05 compared with vehicle-treated mice within each mouse strain.

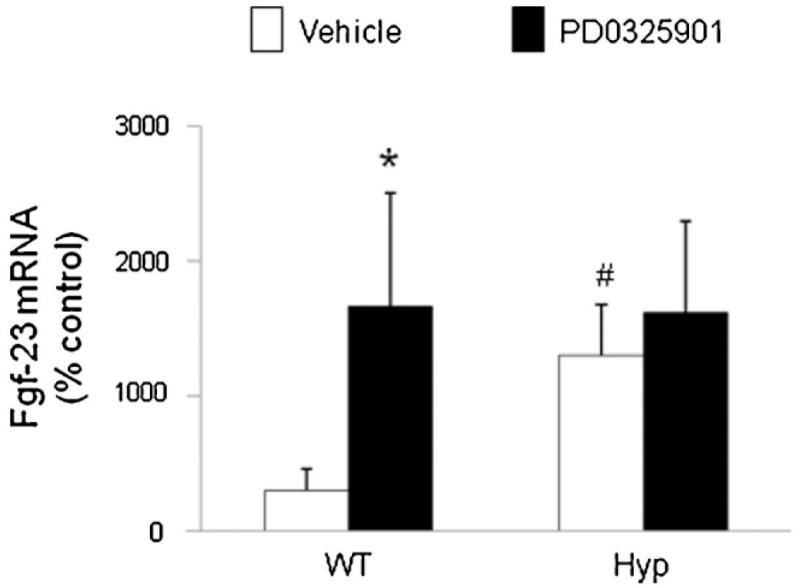

Fig. 7.

Effects of MEK inhibition by PD0325901 on *fgf23* mRNA in bone in wild-type and *Hyp* mice. Mice were administered PD0325901 or vehicle for 4 days. Femoral bone *fgf23* mRNA abundance was quantitated by real-time PCR, normalized to that of *Gapdh* mRNA, and expressed as a percent relative to vehicle-treated mice. Bars depict mean ± SEM (n =7 to 12 mice/group) $^{\#}p$ <.05 compared with wild-type mice within each treatment group. $^{*}p$ <.05 compared with vehicle-treated mice within each mouse strain.